THE JOURNAL OF PHYSICAL CHEMISTRY B

ARTICLE

pubs.acs.org/JPCB

Long-Distance FRET Analysis: A Monte Carlo Simulation Study

Piotr Bojarski,[*,†] Leszek Kulak,[‡] Katarzyna Walczewska-Szewc,[†] Anna Synak,[†] Vincenzo Manuel Marzullo,[§,∥] Alberto Luini,[§] and Sabato D'Auria[*,∥]

[†]Molecular Spectroscopy Division, Institute of Experimental Physics, University of Gdańsk, Wita Stwosza 57, 80-952 Gdańsk, Poland

[‡]Department of Theoretical Physics and Quantum Informatics, Faculty of Technical Physics and Applied Mathematics, Gdańsk University of Technology, Narutowicza 11/12, 80-233 Gdańsk, Poland

[§]TIGEM, Via Pietro Castellino, 111 80131 - Naples, Italy

[∥]Institute of Protein Biochemistry, CNR, Via Pietro Castellino 111 80131 - Naples, Italy

ABSTRACT: A new method for extending the utilizable range of Förster resonance energy transfer (FRET) is proposed and tested by the Monte Carlo technique. The obtained results indicate that the efficiency of FRET can be significantly enhanced at a given distance if the energy transfer takes place toward multiple acceptors that are closely located on a macromolecule instead of a single acceptor molecule as it is currently used in FRET analysis. On the other hand, reasonable FRET efficiency can be obtained at significantly longer distances than in the case of a single acceptor. Randomly distributed and parallel orientated acceptor transition moments with respect to the transition moment of the donor molecule have been analyzed as two extreme cases. As expected, a parallel orientation of donor and acceptor transition moments results in a more efficient excitation energy transfer. This finding could be used to directly reveal the assembly/deassembly of large protein complexes in a cell by fluorescence microscopy.

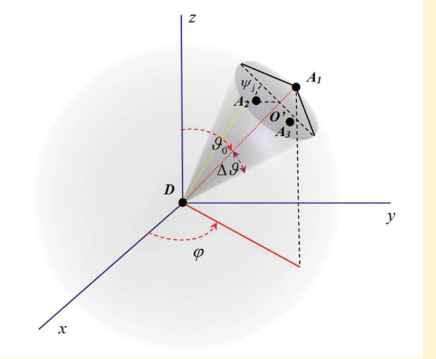

INTRODUCTION

Förster resonance energy transfer[1] (FRET) has become a powerful tool to determine intramolecular distances and molecular conformation variations of bio/molecules.[2] In fact, FRET may act as a spectroscopic ruler for measuring distances not exceeding 10 nm.[3] This property of FRET has been used extensively to study protein−protein interactions in mammalian cells. Cellular functioning is mediated by the activity of many protein complexes that constitute the cellular machines, which drive essentially all life processes including, for example, messenger RNA (mRNA) splicing, vesicle transport, cell migration, and signal transduction. All these basic processes have in common that they involve multiprotein complexes with many components and tight spatial-temporal regulation of protein complexes. Unfortunately, many if not most complexes have sizes above 10 nm. These have been analyzed so far by biochemical methods such as yeast two-hybrid, tandem affinity purification, and mass spectrometry, as well as co-immunoprecipitation and protein-fragment complementation assays (PCAs),[4−6] but not in intact cells. Therefore, our current understanding of these multicomponent systems is limited because of a lack of tools for characterizing their function in the cellular context where they perform their functions.[7]

It would thus be extremely important to investigate many biological processes at distances over 10 nm. A possibly relevant development in this regard has been the emergence of several super-resolution microscopy techniques.[8] These can be used to analyze the molecular distribution patterns in cells, and they have indeed revealed that proteins assemble in defined groups (clusters).[9] Nevertheless, the approach of choice to reveal protein complexes remains the use of FRET, and there is a worldwide interest in the development of new methodologies that allow the use of FRET at longer distances than the present ones.[10,11]

Recently, some of us have shown that the presence of nanostructured silver islands in the proximity of fluorophores contributes to the distance extension of the FRET phenomenon.[12] In particular, it was shown that the effects of metallic silver island films on resonance energy transfer (RET) between the donor 4,6-diamidino-2-phenylindole (DAPI) and the acceptor propidium iodide (PI), both of them bound to a double-helical DNA molecule, resulted in a dramatic increase of the Förster distance from 3.5 nm to an apparent value of 16.6 nm.[13] This finding prompted several researchers to develop new types of FRET-based immunoassays.[14,15] However, the use of silver nanoparticles has a severe restriction for in vivo studies. This is because of the difficulty of introducing silver-labeled fluorescence proteins into the cell and the poisoning action of silver nanoparticles on the cell cycle. Consequently, it appears to be important to develop a metal-free method that allows the use of FRET over longer distances than those presently accessible to investigate the assembly/disassembly of large protein complexes directly in cells.

Received: March 7, 2011
Revised: July 21, 2011
Published: July 22, 2011

The idea of extending the utilizable range of FRET by using the multiple acceptor molecules is possible to realize. Introductory experimental tests have shown that the use of two or three acceptors leads to an increase of the energy transfer efficiency.[16]

Our working hypothesis is based on the use of several rather closely placed acceptors that are bound to a single bio/macromolecule (e.g., an antibody 1) and can amplify energy transfer as an antenna system. Close localization of acceptors means that the acceptor−acceptor distance is only a fraction of the donor−acceptor distance and that the individual differences between particular donor−acceptor distances are insignificant. This condition enables determination of the distance between selected labeled sites on interacting macromolecules with a reasonable accuracy. Acceptors will collect excitation energy that is transferred to them from a single donor molecule localized at a different bio/macromolecule (e.g., an antibody 2).

Further extension of the range of energy transfer can be obtained by preferential nonrandom distribution of acceptor transition moments toward the donor transition moment in emission. In most works devoted to applications of energy transfer in biologically active systems, it is assumed that transition moments of interacting fluorophores are randomly distributed in space (either immobile or fast rotating transition moments). This fact leads to a rather narrow range of the averaged orientation factor values [0.476; 2/3], which limit the application of FRET as a tool to study larger molecular assemblies. However, it follows from the definition of the critical distance that the enhanced value of $\langle\kappa^2\rangle$ can lead to significantly increased value of critical distance for energy transfer. Therefore, it is interesting to study cases of either macroscopically ordered donor−acceptor systems or preferential mutual molecular donor−acceptor orientations at the molecular scale. Such cases appear often in systems with restricted geometries such as biological membranes, photosynthetic units, or quantum dots surrounded by acceptors.[17−19] Nonrandom distribution of donor−acceptor systems leading to enhanced $\langle\kappa^2\rangle$ have been also recently analyzed in the case of partly ordered polymer films.[20]

The Monte Carlo simulations of relative donor quantum yield and fluorescence decays show that the usable range of FRET can be extended even up to 20 nm if multiple acceptors are used and $\langle\kappa^2\rangle$ is high. The results obtained by Monte Carlo studies support our hypothesis indicating that the operating range of FRET can be markedly extended by placing multiple closely located acceptors onto a macromolecule.

MATERIALS AND METHODS

Theoretical Basis. Let us denote the donor molecule D and the ith acceptor molecule A_i . The dynamics of the system considered in the presence of energy transfer is given by

$$\frac{dP_D(\vec{r},t)}{dt} = -\frac{1}{\tau_{0D}}P_D(\vec{r},t) - \sum_{i=1}^{N_A} w^{DA_i}(\vec{r})P_{A_i}(\vec{r},t) \quad (1)$$

with the initial condition

$$P_D(\vec{r},0) = 1, \quad P_{A_i}(\vec{r},0) = 0, \quad i = 1,...,N_A \quad (2)$$

where $P_D(\vec{r},t)$ and $P_A(\vec{r},t)$ denote the probability of finding excitation on a donor D and acceptor A, respectively, at time t and at a fixed molecular configuration, τ_{0D} is the mean fluorescence lifetime of the donor in the absence of energy transfer, and N_A is the number of acceptors in the system.

Förster transfer rate from the excited donor to the ith acceptor molecule is given by

$$w^{DA_i}(r) = \frac{1}{\tau_{0D}}\left(\frac{R_0^{DA}}{r_i}\right)^6 \quad (3)$$

where

$$R_0^{DA} = \left[\frac{9\langle\kappa^2\rangle(\ln 10)\eta_{0D}}{128\pi^5 n^4 N'} I_\nu(D,A)\right]^{1/6} \quad (4)$$

denotes the critical distance for energy transfer from donor to acceptor, and r_i is the distance from the donor to the ith acceptor.

$$I_\nu(D,A) = \int_0^\infty f_D(\nu)\varepsilon_A(\nu)\frac{d\nu}{\nu^4} \quad (5)$$

is the overlap integral, η_{0D} is the absolute donor fluorescence quantum yield in the absence of acceptor, n is the refractive index of the medium, and N' is the number of molecules per 1.0 mmol.

It is worth noting that, in the absence of back energy transfer from excited acceptors to donors, the energy migration to the acceptor ensemble does not affect the donor characteristics; therefore the donor fluorescence intensity decays and its fluorescence quantum yield do not depend on the critical radius R_0^{AA} that describes energy transfer processes among acceptors.

Let us assume the acceptor molecules are distributed in such a way that their distances from the excited donor molecule are approximately the same, i.e., $r_1 \approx r_2 \approx ... \approx r_{NA} = R_{DA}$. Equation 1 with condition 2 and rate constant 3 can be solved yielding the donor fluorescence intensity decay $I_D(t)$ in the following form, after averaging over all possible acceptor configurations:

$$I_D(t) = I_D(0)\exp\left[-\frac{t}{\tau_{0D}} - N_A\frac{t}{\tau_{0D}}\left(\frac{R_0^{DA}}{R_{DA}}\right)^6\right] \quad (6)$$

and the relative donor molecule fluorescence quantum yield:

$$q_D/q_{0D} = \frac{1}{\tau_{0D}}\int_0^\infty I_D(t)\,dt = \frac{1}{1 + N_A\left(\frac{R_0^{DA}}{R_{DA}}\right)^6} \quad (7)$$

where N_A is the number of acceptors. The case considered is formally equivalent to the set of acceptors present on a sphere of a radius R_{DA} and the donor molecule located in the center of the sphere. In the simple case of N_A= 1 and $R_0^{DA} = R_{DA}$, the relative donor fluorescence quantum yield is 0.5, whereas in the absence of acceptors, q_D/q_{0D} is equal to 1 and no fluorescence intensity decay occurs.

Monte Carlo Simulation. Let us now assume the acceptor molecules A_1, A_2, ..., A_{NA} are placed randomly on a surface of a cone as presented in Figure 1 describing the geometry of the simulated system. Additionally, the Monte Carlo method can be rather easily extended to different topologies and further effects such as homotransfer.[21,22] The angles φ, ϑ, and $\Delta\vartheta$ are necessary to define the locations of acceptor molecules. First, we randomly choose the angle ϑ_0 between the cone axis and the z axis from Cartesian coordinate system (cp. Figure 1). Next, according to the maximal distance between acceptors, we calculate the

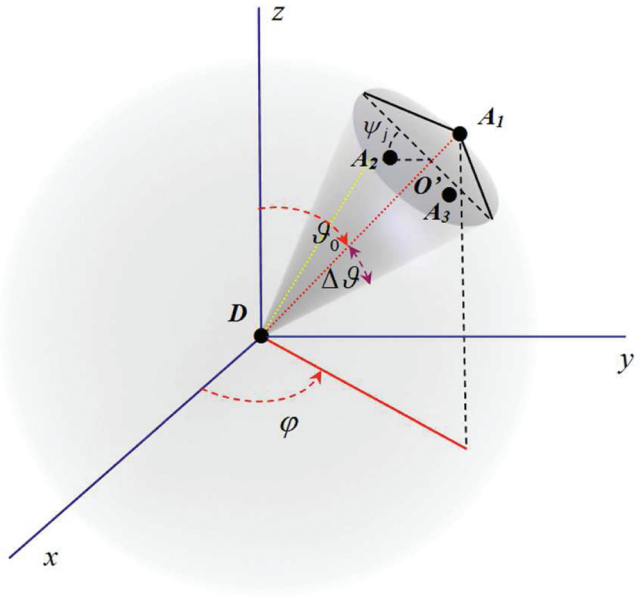

Figure 1. Geometric relations for donor−multiple acceptor system. D and A denote donor molecule and acceptor molecule, respectively; the angles φ, ϑ_0, and $\Delta\vartheta$ define the location of a given acceptor molecule.

appropriate angle $\Delta\vartheta$. In the next step we randomly choose the value of angle ϑ_j, from the interval $[\vartheta_0 - \Delta\vartheta, \vartheta_0 + \Delta\vartheta]$, which is one of the jth acceptor coordinates in the spherical coordinate system, i.e., $\vec{r}$ = (RDA, ϑ_j, ψ_j). The value of the angle ψ^j is obtained by randomly choosing the number from the interval $[0,2\pi]$.

During calculation of the acceptors configuration, the cutoff radius was introduced to avoid the appearance of statistical pairs, i.e., for distances between two acceptors that are shorter than a certain physically accepted value (typically dye molecular radius, i.e., 0.5 nm): this kind of configuration was not considered.

The algorithm used (Metropolis algorithm) consists of the employment of the random-number generator for the cyclic formulation of answers to two questions: (1) When do any of the preset luminescent processes take place in the simulated system? and (2) What kind of process is it?[21,22] The Monte Carlo simulation is organized as follows: at first, the primarily excited donor molecule is placed in the center of a sphere, which represents the simulated system.

(1) The excited donor molecule can be deactivated through the following processes:

(P_1) process 1: D* → D, photon emission or nonradiative energy conversion, with the rate $1/\tau_{0D}$;

(P_2) process 2: D* + A → D + A*, nonradiative energy transfer from the excited donor to an acceptor, with the transfer rate w^{DA};

(P_3) process 3: D* + D → D + D*, nonradiative energy homotransfer from the excited donor to an unexcited donor, with the transfer rate w^{DD};

(2) Next, the values of the following total transfer rates are calculated:

$$c_1 = 1/\tau_{0D} \quad c_2 = \sum_{i=1}^{N_A} w^{DA_i} \quad c_3 = \sum_{i=1}^{N_D} w^{DD_i} \tag{8}$$

where N_A and N_D are the numbers of acceptors and donors in the system, respectively.

(3) Next, the time moment at which any of the investigated processes occurs is calculated by inverting the distribution function of the probability, $p(t,P_k)\,dt$, so that if at time t the donor molecule is excited, then the process P_k appears in the time interval $(t, t + dt)$:

$$p(t) = \sum_{k=1}^{3} p(t, P_k) = c\exp(-ct) \tag{9}$$

where

$$c = c_1 + c_2 + c_3 \tag{10}$$

For this purpose a random number r_1 is generated, and the time at which any process takes place is obtained by inverting the distribution function of the probability $p(t)$,

$$\int_0^t \mathrm{p}(t)\,dt = r_1, \text{ i.e., } t = -(1/c)\ln(1 - r_1) \tag{11}$$

(4) In this step it is determined which process took place at time t. By generating the next random number, r_2, such a value of index k can be found for which the following inequality is satisfied:

$$\sum_{i=1}^{k-1} c_i < r_2 c \le \sum_{i=1}^{k} c_i, \quad k = 1, 2, 3 \tag{12}$$

If k = 1, then the activated molecule is quenched by a photon emission or nonradiative excitation energy conversion, and if k = 2 or 3, the energy transfer or homotransfer process takes place, respectively. The simulation run is finished when excitation is taken from the donor ensemble. Next, a new simulation step can run.

The relative donor quantum yield is calculated by dividing the number of simulation runs finished with the donor emission by the number of all runs.

The histogram of fluorescence decay is calculated based on the following equation:

$$\Phi_D(\Delta t_k) = 1 - \left(\sum_{j=1}^{k} n_j / \sum_{j=1}^{k_{max}} n_j\right) \tag{13}$$

where $\Delta t_k = (k/k_{max})t$, k_{max} is the number of histogram intervals, and n_j is the number of donor deactivations.

During the simulation, instead of assuming averaged values of the orientation factor, we calculated the real values for any pair of interacting molecules. In addition, the averaging analysis was performed over a suitably high number of simulation runs. To obtain well averaged results, Monte Carlo simulations were repeated 10^7 times (10^7 molecular configurations).

RESULTS AND DISCUSSION

In order to determine the intramolecular distance, we assume that acceptors A are separated from a single donor D by an approximately equal distance, and the A−A distance is significantly shorter than the D−A distance. In addition, it is assumed that acceptors do not form aggregates. In the case of aggregate formation, the presence of additional quenching centers should be considered, and the Monte Carlo procedure should be extended to describe FRET in a three-component system. Such considerations have been performed in some of our previous works in the case of solutions and isotropic and anisotropic

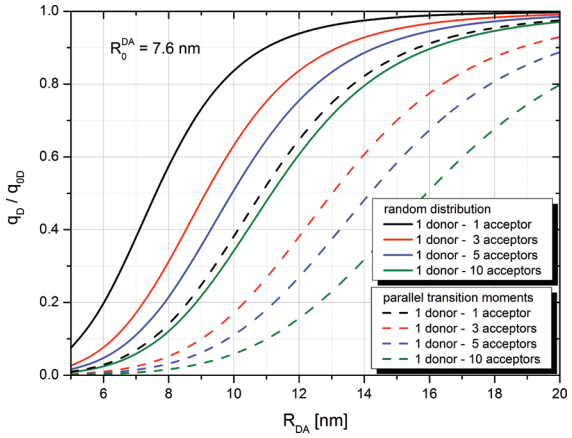

Figure 2. Relative donor fluorescence quantum yield in the presence of multiple acceptors for a random and parallel orientation of all molecules.

polymer films,[20−23] and they can be adopted to extend procedures considered in the current work if necessary for any application.

Now, we will focus on two different cases: (1) A molecules are randomly oriented with an immobile transition moments of interacting molecules; (2) molecular transition moments of the A molecules are fixed with a parallel orientation. The proposed method can be also applied to partly ordered systems[20] (for a given distribution function of transition moments or for experimentally defined spatial distribution of transition moments), and it can be used to more realistically describe selected systems important from a biological or biophysical point of view.

To analyze the effect of the number of cumulated acceptors on the efficiency of energy transfer, Monte Carlo simulations were performed for different numbers of acceptors upon energy transfer.

Figure 2 shows the dependence of the relative donor fluorescence quantum yield in the presence of acceptors as a function of donor−acceptor separation in two cases: random angular distribution of all molecular transition moments, and parallel orientation of all transition moments ($\langle\kappa^2\rangle = 4$). It can be seen from Figure 2 that the optimal conditions for energy transfer corresponding to 50% transfer efficiency ($q_D/q_{0D} = 0.5$) shift significantly with the number of acceptors able to collect excitation energy from the donor molecule. For random orientation of transition moments in the case of a single donor−single acceptor system, this condition corresponds to $R_{DA} = 7.6$ nm, whereas for 1 donor−10 acceptors it relates to $R_{DA} = 11.2$ nm. This example shows how it is possible to extend the useful range of energy transfer as a spectroscopic ruler. In fact, still accurate determination of separation distance can be found for somewhat lower energy transfer efficiency (higher donor fluorescence quantum yield), which, as seen from the figure, is possible even for $R_{DA} \cong 15$ nm for systems with 1 donor and 10 acceptors. From Figure 2 it is also possible to say that it is important to consider some cases of nonrandomly mutually oriented donor and acceptor molecules. Let us, for example, consider the case of a single donor and a set of acceptors, the transition moments of which are mutually parallel. Due to the angular correlations between acceptor molecules, they act as a powerful antenna system and collect more efficiently excitation energy from the donor molecule. Indeed, as seen from the Figure 2, this allows larger D−A separation to be determined. For the corresponding system of 1 donor and 10 acceptors, it seems possible to determine distances as long as $R_{DA} \cong 20$ nm.

Figure 3a−d shows that donor fluorescence intensity decays in the presence of acceptors for a couple of donor−acceptor separations. Again, two cases were considered: (a) the random distribution of acceptors; (b) the parallel alignment of molecular transition moments. The critical distance in the system considered is 7.6 nm. For a separation distance $R_{DA} = 5$ nm significantly shorter than the critical one, it can be seen that the donor fluorescence decay is very fast due to extremely effective energy transfer (Figure 3a,b). In the case of 5 or 10 acceptors, the decays for this separation are even faster (data not shown). However, an interesting observation can be made when looking at fluorescence intensity decay curves corresponding to the longest donor−acceptor separations: 12.5 and 14 nm in the case of random orientation. For a small number of acceptors, these curves are almost indistinguishable, indicating that energy transfer cannot act as a spectroscopic ruler at such long distances.

However, as the number of acceptor molecules increases, the resolution between both curves improves, and it is evident that for 5 acceptors it is possible to measure distances over 10 nm long. Similar considerations can be made for donor fluorescence intensity decays if transition moments of acceptors are mutually parallel and are also parallel to the donor transition moment. In this case, one can anticipate even higher resolution between the previously described decay curves. Indeed, the results presented in Figure 3a−d fully confirm these expectations. Even for a single donor−acceptor pair, the decay curves corresponding to 12.5 and 14.0 nm separation distance are easily distinguishable.

It also occurs that the presence of homotransfer (several donors exchanging excitation energy) does not affect the fluorescence donor quantum yield or its fluorescence decay curve, but it strongly accelerates the decay of primarily excited donors (emission anisotropy decay).

The lack of homotransfer effect on the donor quantum yield and its intensity decay is due to the full compensation of two effects: (1) the shortening of the mean localization time of excitation on donor molecules and (2) the increased number of excitation jumps within the set of donors compared to the case of single donor−single acceptor system. An example of the influence of homotransfer on the decay of primarily excited molecules (emission anisotropy decay) is given in Figure 4. We assumed the critical distance for homotransfer $R_0^{DD} = 5$ nm, which is a typical value for many dyes. It can be seen from Figure 4 that the increasing number of donors leads to strong acceleration of the decay of primarily excited molecules.

FINAL REMARKS

The usable range of FRET can be extended by placing multiple closely located acceptor molecules onto a bio/macromolecule. Further manipulations and extensions of FRET range are possible, if the transition moments of donor and acceptor molecules are not random.

Mention should be made that for multiple closely located acceptors or donors, dimer formation and self-quenching effect can occur, effects well-known and thoroughly studied in concentrated solutions.[23−25] If dimers are formed, the system becomes multicomponent, and the presence of additional quenching centers has to be taken into account in the simulation procedure. Such an extended procedure for three- or four-component systems has been described earlier by us in the case of concentrated Rhodamine B solutions, where the presence of zwitterion and cationic forms of the dye as well as dimers of both

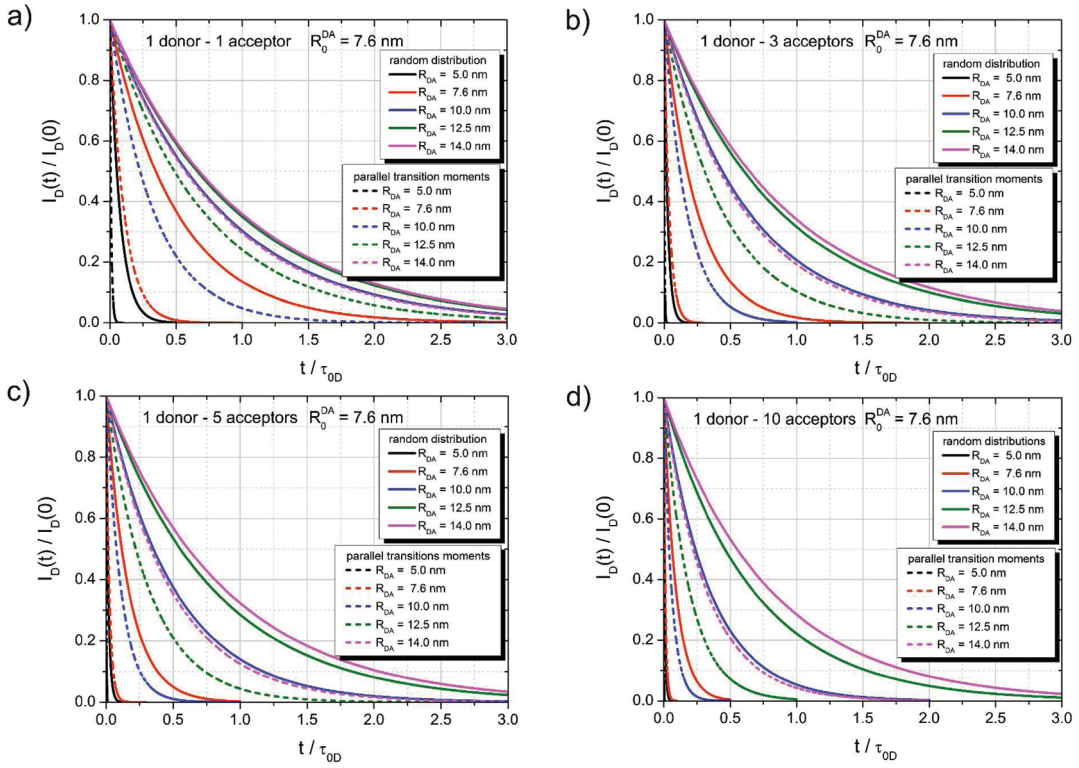

Figure 3. Donor fluorescence intensity decay (a–d) in the presence of multiple acceptors for a random and parallel orientation of all molecules. (a) 1 donor–1 acceptor; (b) 1 donor–3 acceptors; (c) 1 donor–5 acceptors; (d) 1 donor–10 acceptors.

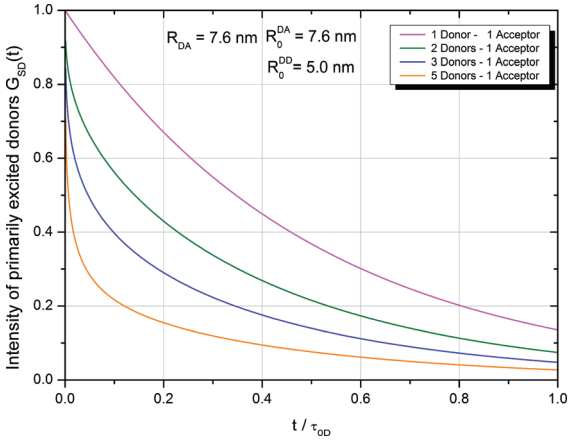

Figure 4. Fluorescence decay of primarily excited donors for different numbers of donors and for a single acceptor (random distribution).

forms have been found, and a good correspondence between simulation results of the concentration quenching and experimental data has been obtained.[23] Three-component highly ordered fluorescent systems have been also studied by us in terms of Monte Carlo simulations in the case of uniaxially stretched polymer films doped with three fluorescent dyes forming a donor–mediator–acceptor system.[20] Therefore, generalization of the Monte Carlo algorithm to describe multiple acceptor types linked to proteins is possible.

However, we would like to point out that from the experimental point of view it may advisible to limit the number of acceptors in order to prevent aggregation while keeping the energy transfer efficiency high. The highest advisible number of acceptors will depend on several factors, such as (a) the size of a macromolecules and fluorophores; (b) the macromolecule susceptibility to dimerize and/or to aggregate; and (c) the number of reactive sites present on the macromolecules. In addition, it should also be mentioned that self-quenching and energy homotransfer may be considered as two separate phenomena.[26] In fact, dimer formation leading to self-quenching requires much shorter intermolecular distances than those needed to observe excitation homotransfer (exclusively through fluorescence depolarization, but not any change in the quantum yield). Usually, the self-quenching phenomenon is preceded by the homotransfer phenomenon, and it occurs as the final step of energy transfer to the aggregate. It should also be noted that from an experimental point of view it is easy to distinguish the two different phenomena by performing time-resolved fluorescence depolarization and fluorescence mean-lifetime measurements.

Finally, we would like to highlight that the labeling reaction of macromolecules by fluorescence acceptors will certainly lead to a nonintegral mean number of acceptors on the macromolecules. However, independently of the used function for the calculations, the close localization of the acceptors will result in a narrow profile of the distribution function and small uncertainty of the mean R_{DA}.

AUTHOR INFORMATION

Corresponding Author

*(P.B.) Address: University of Gdańsk, Institute of Experimental Physics, Wita Stwosza 57, 80-952 Gdańsk, Poland; e-mail: fizpb@ug.edu.pl. (S.D.) Address: CNR-IBP Via Pietro Castellino, 111 80131 Napoli, Italy; tel. +39-0816132250; fax: + 39-08-16132312; e-mail: s.dauria@ibp.cnr.it.

■ ACKNOWLEDGMENT

This project is in the framework of the CNR Commessa" Diagnostica Avanzata" (S.D.) and NR 15 0029/2009 (P.B.). This research has been partially supported within the International Ph. D. Project (MPD/2009-3/4) financed by the Foundation for Polish Science (K.W.S.) and Human Capital Operational Programme, Action 4.1.1 "Educators for the Elite - integrated training program for Ph.D. students, Post-docs and Professors as academic teachers at University of Gdańsk" (A.S.). S.D. and P.B. thank Prof. Ignacy Gryczynski and Zygmunt Karol Gryczynski for the valuable suggestions and the long discussions on the topic of the work.

■ REFERENCES

(1) Förster, Th. *Ann. Phys.* **1948**, *2*, 55.
(2) Lakowicz, J. R. *Principles of Fluorescence Spectroscopy*, 3rd ed.; Springer Verlag: Berlin, 2006.
(3) Stryer, L.; Haughland, R. P. *Proc. Natl. Acad. Sci. U.S.A.* **1967**, *58*, 719.
(4) Shoemaker, B. A.; Panchenko, A. R. *PLoS Comput. Biol.* **2007**, *3*, 337–344.
(5) Shoemaker, B. A.; Panchenko, A. R. *PLoS Comput. Biol.* **2007**, *3*, 595–601.
(6) Arkin, M. R.; Wells, J. A. *Nat. Rev. Drug Discovery* **2004**, *3*, 301–317.
(7) Piljić, A.; Schultz, C. *ACS Chem. Biol.* **2008**, *3* (12), 749–55.
(8) Hell, S. W. *Science* **2007**, *316* (5828), 1153–8.
(9) Lang, T.; Rizzoli, S. O. *Physiology (Bethesda).* **2010**, *2*, 116–24.
(10) Pope, A. J.; Haupts, U. M.; Moore, K. J. *Drug Discovery Today* **1999**, *4*, 8.
(11) Saini, S.; Srinivas, G.; Bagchi, B. *J. Phys. Chem. B* **2009**, *113*, 1817–1832.
(12) Lakowicz, J. R.; Shen, Y.; D'Auria, S.; Malicka, J.; Gryczynski, Z.; Gryczynski, I. *Anal. Biochem.* **2002**, *301*, 267–277.
(13) Lakowicz, J. R.; Kusba, J.; Shen, Y.; Malicka, J.; D'Auria, S.; Gryczynski, Z.; Gryczynski, I. *J. Fluoresc.* **2003**, *13* (1), 69–77.
(14) Matveeva, E.; Gryczynski, Z.; Malicka, J.; Gryczynski, I.; Lakowicz, J. R. *Anal. Biochem.* **2004**, *334*, 303–311.
(15) Staiano, M.; Matveeva, E. G.; Rossi, M.; Crescenzo, R.; Gryczynski, Z.; Gryczynski, I.; Iozzino, L.; Akopova, I.; D'Auria, S. *ACS Appl. Mater. Interfaces* **2009**, *1* (12), 2909–16.
(16) Koushik, S. V.; Blank, P. S.; Vogel, S. S. *PloS One* **2009**, *4* (11), e8031.
(17) Van der Meer, W. *Excitation Energy Transport in Restricted Geometries*; Springer Verlag: Berlin, 1994.
(18) Algar, W. R.; Krull, U. J. *Anal. Bioanal. Chem.* **2010**, *398*, 2439–2449.
(19) Cheng, Y.-C.; Fleming, G. R. *Annu. Rev. Phys. Chem.* **2009**, *60*, 241–262.
(20) Bojarski, P.; Sadownik, M.; Rangełowa-Jankowska, S.; Kułak, L.; Dasiak, K. *Chem. Phys. Lett.* **2008**, *456*, 166–169.
(21) Rangelowa-Jankowska, S.; Kulak, L.; Bojarski, P. *Chem. Phys. Lett.* **2008**, *460*, 306–310.
(22) Kulak, L. *Chem. Phys. Lett.* **2008**, *457*, 259–262.
(23) Bojarski, P.; Jankowicz, A. *J. Lumin.* **1999**, *81*, 21–31.
(24) Grajek, H.; Gryczynski, I.; Bojarski, P.; Gryczynski, Z.; Bharill, S.; Kułak, L. *Chem. Phys. Lett.* **2007**, *439*, 151–156.
(25) Synak, A.; Kułak, L.; Rangełowa-Jankowska, S.; Grobelna, B.; Kubicki, A.; Bojarski, P. *Chem. Phys.* **2011**, *382*, 47–51.
(26) Bojarski, P.; Kułak, L.; Bojarski, C.; Kawski, A. *J. Fluoresc.* **1995**, *5*, 293–306.